Colloids and Surfaces A: Physicochemical and Engineering Aspects 631 (2021) 127639

Contents lists available at ScienceDirect

Colloids and Surfaces A: Physicochemical and Engineering Aspects

journal homepage: www.elsevier.com/locate/colsurfa

Size-controlled nanoscale octahedral HKUST-1 as an enhanced catalyst for oxidative conversion of vanillic alcohol: The mediating effect of polyvinylpyrrolidone

Bing-Cheng Li [a,1], Jia-Yin Lin [a,1], Jechan Lee [b], Eilhann Kwon [c], Bui Xuan Thanh [d], Xiaoguang Duan [e], Hsing Hua Chen [a], Hongta Yang [f,*], Kun-Yi Andrew Lin [a,*]

[a] Department of Environmental Engineering & Innovation and Development Center of Sustainable Agriculture, National Chung Hsing University, 145 Xingda Rd., South Dist., Taichung City 402, Taiwan
[b] Department of Environmental and Safety Engineering, Ajou University, Suwon 16499, Republic of Korea
[c] Department of Environment and Energy, Sejong University, 209 Neungdong-ro, Gunja-dong, Gwangjin-gu, Seoul, Republic of Korea
[d] Faculty of Environment and Natural Resources, Ho Chi Minh City University of Technology, VNU-HCM, 268 Ly Thuong Kiet, District 10, Ho Chi Minh City 700000, Viet Nam
[e] School of Chemical Engineering and Advanced Materials, The University of Adelaide, SA 5005, Australia
[f] Department of Chemical Engineering, National Chung Hsing University, 145 Xingda Rd., South Dist., Taichung City 402, Taiwan

GRAPHICAL ABSTRACT

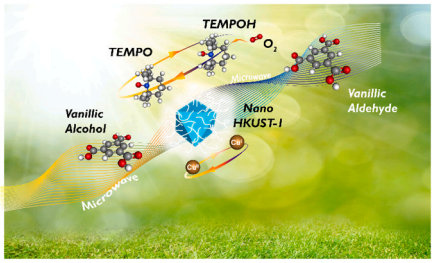

ARTICLE INFO

Keywords:
HKUST-1
Polyvinylpyrrolidone
2,2,6,6,-Tetramethylpiperidine 1-oxyl
Vanillic alcohol
Lignin
Vanillic aldehyde

ABSTRACT

While 2,2,6,6-tetramethylpiperidin-oxyl (TEMPO) accompanied with Cu is a promising oxidative catalytic process for converting vanillic alcohol (VL), to vanillic aldehyde (VE), the Cu-based metal organic frameworks (MOFs), HKUST-1, appears as a useful heterogeneous catalyst for VL conversion. Nevertheless, since the typical HKUST-1 is micrometer-scaled, it would be more advantageous to make HKUST-1 into nanoscale to increase outer surfaces of HKUST-1. Thus, the goal of this study is to develop a useful approach to prepare nanoscale HKUST-1 which can still exhibit octahedral morphology. Specifically, nano-HKUST-1 is developed here via mediation by polyvinylpyrrolidone (PVP). These PVP-mediated nano-HKUST-1 not only retains the crystalline structure of HKUST-1 but also maintains the octahedral morphology of HKUST-1. Interestingly, the introduced PVP would not just alter the size of HKUST-1 but also deposit PVP molecules into these nano-HKUST-1, increasing hydrophilicity of nano-HKUST-1 to attract VL in solvents. Thus, nano-HKUST-1 could exhibit noticeably higher VL conversion efficiencies then the conventional HKUST-1 owing to the smaller size, and the

* Corresponding authors.
E-mail addresses: hyang@nchu.edu.tw (H. Yang), linky@nchu.edu.tw (K.-Y.A. Lin).
[1] These authors contribute equally to the study.

https://doi.org/10.1016/j.colsurfa.2021.127639
Received 27 May 2021; Received in revised form 22 September 2021; Accepted 24 September 2021
Available online 29 September 2021

more hydrophilic surficial properties. Moreover, nano-HKUST-1 could also exhibit a high Y_{VE} = 91% with S_{VE} = 100% at 120 °C for 120 min, outperforming many other reported values. Nano-HKUST-1 can be also reusable and exhibit stable Y_{VE} and 100% of S_{VE}. These features all indicate that nano-HKUST-1 prapred by mediation of PVP is a more advantageous Cu-based catalyst for converting VL to VE, and the mediating effect of PVP revealed here also gives insights to further engieer MOFs materials for enhancing their applications.

1. Introduction

Oxidative conversion of vanillic alcohol (VL) represents an interesting and promising process as it could be implemented under environmentally-friendly conditions to generate high-value-added products [1–3], such as vanillic aldehyde (VE), a valuable compound consumed broadly in perfumes, foods, cosmetics, and pharmaceuticals [4–7]. Nevertheless, the conversion of VL into VE would necessitate a particular oxidation of alcohol moiety of VL into an aldehyde moiety; therefore, it is very critical to establish highly-effective methods to selectively convert the alcohol moiety of VL into the aldehyde moiety.

While conventional oxidation of VL can be executed by using H_2O_2, H_2O_2, extensive amounts of non-recyclable H_2O_2 would be demanded to achieve stoichiometric chemistry of oxidation [8,9]. More importantly, these H_2O_2-based processes usually lead to very low conversion efficiencies and selectivities of VL to VE [1,10]. Therefore, more effective, and selective oxidative processes are highly desired. As 2,2,6,6-Tetramethylpiperidine 1-oxyl (TEMPO) co-catalyzed with copper (Cu), iron (Fe), and Laccase, has been unveiled as a recyclable oxidation process recently [11–14], Cu/TEMPO has been also validated to effectively oxidize VL to VE [12,15–18]. Moreover, a few heterogeneous-phase Cu catalysts have been also proposed to co-catalyze with TEMPO for oxidizing VL to resolve recovery issues of homogeneous Cu ions [12,18]. In particular, Cu-based metal organic frameworks (MOFs) (i.e., HKUST-1) have been demonstrated as a potential heterogeneous catalyst for oxidizing VL to VE [19–22]. HKUST-1 represents the most extensively-studied MOF, and HKUST-1 is also the most typical Cu-containing MOF. In addition, the synthesis of HKUST-1 is relatively simple and can be prepared under mild conditions [23].

While MOFs usually exhibit high surface areas owing to internal

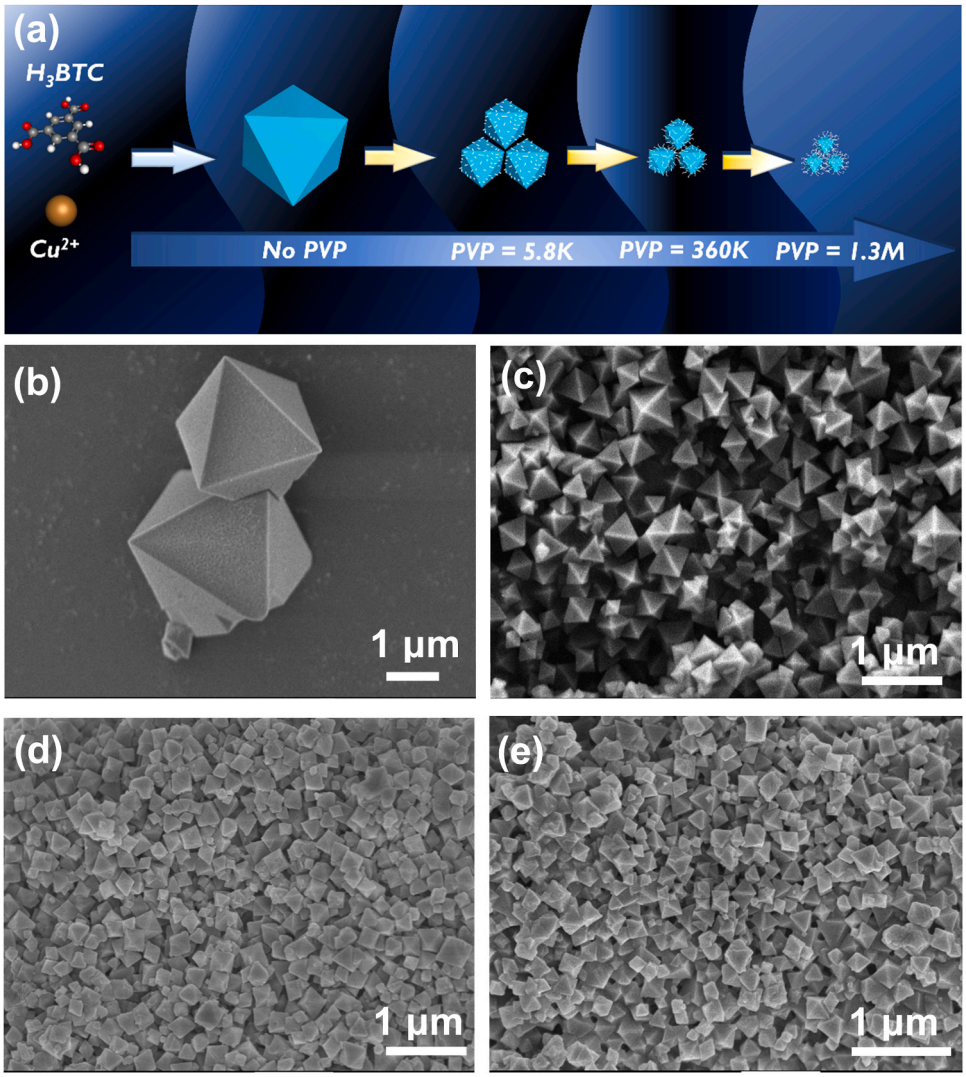

Fig. 1. (a) a preparation scheme of HKUST-1 with various sizes prepared with and without PVP; SEM images of HKUST-1 prepared with and without PVP: (b) HKUST-1 without PVP, (c) nano-HKUST-1 prepared with PVP = 5.8 K, (d) nano-HKUST-1 prepared with PVP = 360 K, and (e) nano-HKUST-1 prepared with PVP = 1.3 M.

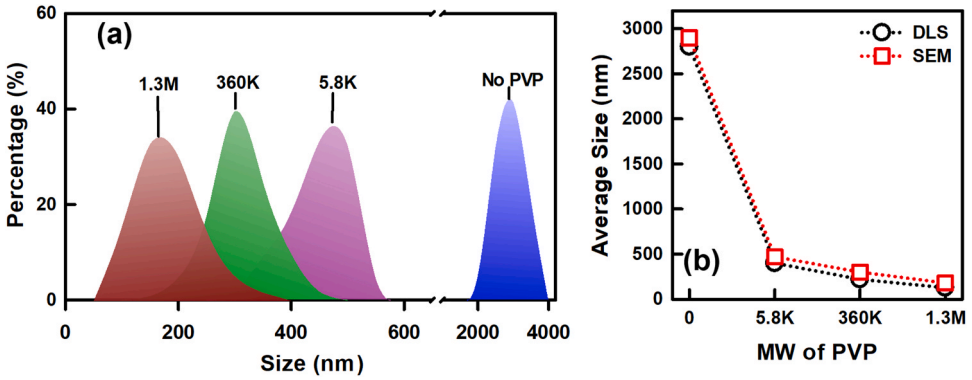

Fig. 2. Particle sizes of HKUST-1, and nano-HKUST-1 determined based on (a) SEM images, and (b) DLS measurements.

spaces [24], MOFs in liquid-phase environments would be saturated with water or solvent molecules [25]. Moreover, sizes of reactants would be also larger than windows of MOFs, and constrain reactions only on outer surfaces of MOFs rather than internal spaces. MOFs with a smaller size with a well-defined shape shall exhibit more outer surfaces exposing to reactants. As the aforementioned HKUST-1 typically exhibits micrometer-scale [26–28], it would be certainly advantageous to make HKUST-1 smaller, especially into nanoscale dimensions. Even though there are several methods to prepare micro-scale HKUST-1[26,28,29], very few studies have ever reported preparation of nanoscale HKUST-1. Wang et al. proposed a coordination modulation method to modulate nucleation and crystal growth processes to afford nanoscale HKUST-1 [30], whereas Li et al. demonstrated an ultrasound-assisted synthesis to result in a nanoscale HKUST-1 [31]. Nevertheless, the nanoscale HKUST-1 obtained by these two studies did not maintain the typical octahedral morphology of HKUST-1, leading to aggregation of HKUST-1 particles [30,31].

Thus, the goal of this study is to develop a useful approach to prepare nanoscale HKUST-1 which can still exhibit octahedral morphology. Specifically, as polyvinylpyrrolidone (PVP) is a stable polymer, and widely used as a capping agent for preparing nanostructures [32,33], PVP shall be a promising additive to enable the formation of nanoscale octahedral HKUST-1. However, almost no studies have been ever reported to employ PVP as an additive to mediate the formation of HKSUT-1 for controlling sizes of HKUST-1. Therefore, this study would be the first study for investigating the synthesis of nano-HKUST-1 via mediation by PVP. As no studies have been also reported for employing PVP-mediated nano-HKUST-1 for converting VL to VE in the presence of TEMPO, this present study would provide valuable information and insight for optimizing HKUST-1 as a heterogeneous catalyst for conversion of VL to VE.

2. Experimental

2.1. Preparation of HKUST-1

All chemicals used in this study were purchased from Sigma-Aldrich (USA), and employed directly without further purification. The conventional HKUST-1 (i.e., micrometer-scaled HKUST-1) was synthesized according to the reported procedure [34,35]. HKUST-1 prepared with and without PVP can be illustrated schematically in Fig. 1(a). The protocol for preparing nano-HKUST-1 was similar to that for the conventional HKUST-1 except that PVP at an equivalent weight of H_3BTC was additionally introduced to mixtures of Cu^{2+} and Benzene-1,3,5-tricarboxylic acid (H_3BTC) during the preparation of HKUST-1. For investigating the influence of PVP on the formation of nano-HKUST-1, MW of PVP was varied from 5800 Da (5.8 K) to 360,000 Da (360 K), and then 1300,000 Da (1.3 M), to afford various nano-HKUST-1 denoted as nano-HKUST-1(5.8 K), nano-HKUST-1(360 K), and nano-HKUST-1 (1.3 M), respectively.

2.2. Characterization of HKUST-1

Morphologies of HKUST-1 and nano-HKUST-1were determined by FE-SEM (JEOL JSM-7800F, Japan). Their XRD patterns were characterized through an X-ray diffractometer (Bruker, USA), and textural properties were measured using a volumetric gas adsorption analyzer (ANTON PAAR NOVATOUCH LX2, Austria). Their FTIR spectra were obtained through using an FTIR spectrometer (Perkin Elmer Spectrum Two, USA). Particle sizes of HKUST-1 and nano-HKUST-1 in solvents were quantified by dynamic light scattering (DLS) zetasizer (Malvern, UK).

2.3. Conversion of VL to VE using HKUST-1

Catalytic oxidation of VL was conducted in a 100 mL of Teflon-lined reactor based on previous reported protocols [8,19,28,36,37]. First, 150 mg of VL and 20 mL of isopropanol were introduced to the Teflon-lined reactor. Subsequently, 100 mg of the as-prepared HKUST-1 and 100 mg TEMPO were added to the VL solution. Then, the resulting mixture was heated in either a conventional oven (Memmert ULE 400, Germany) or a microwave system (Milestone Ethos UP, Italy). After pre-set reaction times, sample aliquots were withdrawn from the reactor and filtrated by syringe membrane disks (0.22 μm, PVDF). The filtrates were analyzed for determining concentrations of reactants and products by a HPLC (Kanuer Azura, Germany) with a UV-Vis detector. The mobile phase was comprised of DI water (79%), acetonitrile (20%) and acetic acid (1%) at a flowrate of 1.0 mL/min.

Conversion efficiency of VL to VE (or other products) was quantified as follows [4,34]:

$$\text{Conversion of VL } (C_{VL}) = \text{Consumed VL/Total VL } (100\%) \quad (1)$$

$$\text{Selectivity for VE } (S_{VE}) = \text{VE/Consumed VL}(100\%) \quad (2)$$

$$\text{Yield } (Y_{VE}) = \text{VE/Total VL } (100\%) \quad (3)$$

3. Results and discussion

3.1. Characterization of HKUST-1

To elucidate the PVP-mediating effect on the morphology of HKUST-1, SEM images of the conventional HKUST-1 and nano-HKUST-1 were firstly determined. Fig. 1(b) presents the conventional HKUST-1 without any addition of PVP, and it exhibited a typical octahedral shape with micrometer-scaled sizes, which were in a good agreement with the reported sizes in the previous studies [38–40]. After introducing PVP = 5.8 K during synthesis of HKUST-1, the resulting HKUST-1

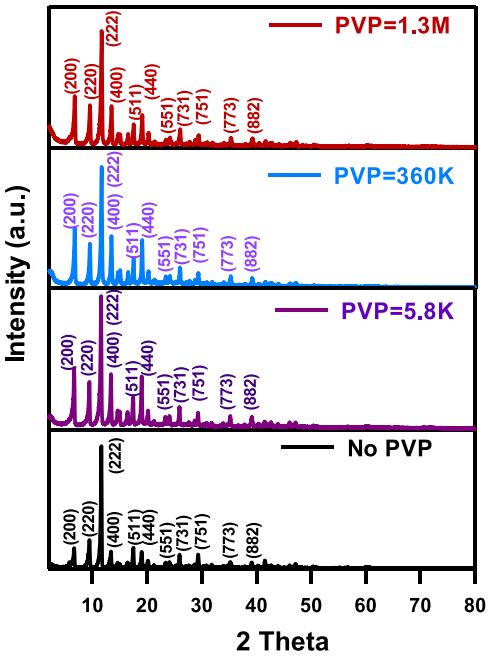

Fig. 3. XRD patterns of HKUST-1, and nano-HKUST-1.

(Fig. 1(c)) could also exhibit the octahedral shape; however, its size had been significantly decreased to be ca. 450–500 nm. When PVP with higher MWs of 360 K and 1.3 M were then introduced, the resultant HKUST-1 particles can still exhibit the octahedral morphologies but their sizes further became even smaller.

To further quantify sizes of these HKUST-1 particles with and without the addition of PVP, SEM images of these HKUST-1 particles were analyzed by determining edge lengths of HKUST-1 octahedrons, and the corresponding size distributions are then displayed in Fig. 2(a). As the conventional HKUST-1 exhibited a micrometer-scaled size ranging from 1.8 to 3.9 μm with an average of 2.9 μm, those HKUST-1 prepared with PVP exhibited considerably smaller sizes which fell into the nanoscale range, forming nano-HKUST-1. In particular, the nano-HKUST-1 prepared with PVP = 5.8 K showed sizes ranging from 300 to 560 nm with an average size of 480 nm, whereas the nano-HKUST-1 prepared with PVP = 360 K exhibited sizes ranging from 160 nm to 470 nm with an average size of 310 nm. Once MW of PVP further increased to 1.3 M, its corresponding size ranged from 50 to 390 nm with an average of 170 nm. The size distributions of the conventional HKUST-1 and nano-HKUST-1 further validated that the introduction of PVP into HKUST-1 would considerably reduce the particle size of HKUST-1, and, more interestingly, a higher MW of PVP would lead to the much smaller size.

Since the aforementioned size distributions of HKUST-1 and nano-HKUST-1 were determined by images of HKUST-1, it would be interesting to further elucidate sizes of HKUST-1 in liquid phase as VL oxidation reaction is conducted in solvents. Thus, the particle sizes of HKUST-1 were further identified by DLS, and displayed in Fig. 2(b), in which the conventional HKUST-1 still exhibited the micrometer-scaled size with an average size of 2800 nm. Interestingly, the sizes determined by SEM images were comparable to the sizes obtained by DLS. Those HKUST-1 prepared in the presence of PVP also exhibited nanoscale sizes and, more importantly, the size of nano-HKUST-1 was also reverse to MW of PVP as a higher MW of PVP led to a much smaller particle size of HKUST-1, validating that the size of HKUST-1 would be manipulated by the addition of PVP with various MWs. As PVP was employed as a capping agent which would prevent aggregation of particles by the steric effect, a higher MW of would lead to a stronger steric effect, rendering the resulting particles smaller [41]. Previous studies

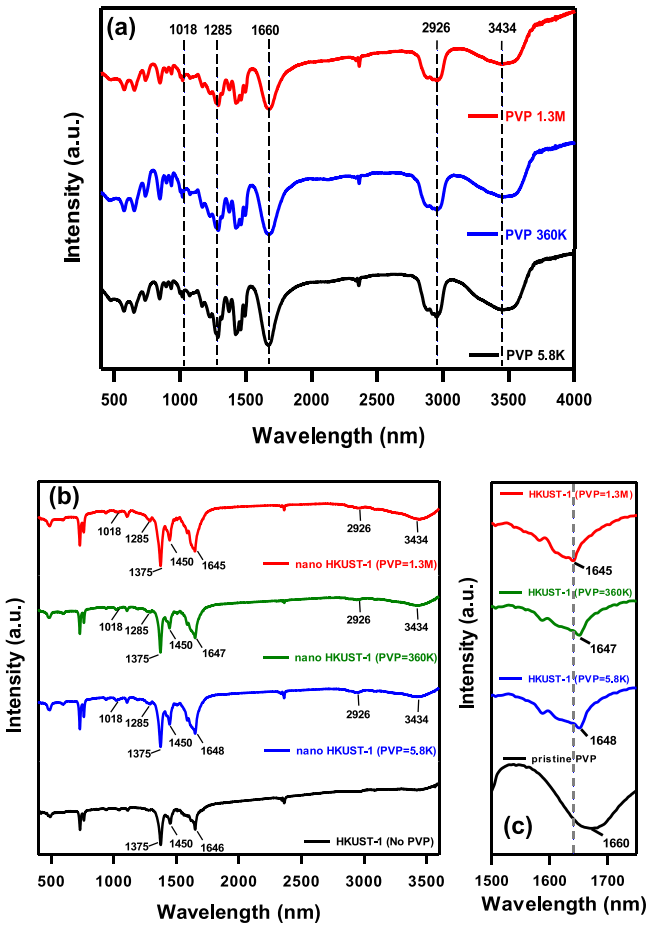

Fig. 4. FTIR spectra of (a) pristine PVP with various MWs, (b) HKUST-1 prepared with and without PVP, and (c) regional spectra of HKUST-1 prepared with and without PVP.

have also revealed that when the viscosity of the precursor solution increased, a higher MW of PVP would also cause the precursor solution to be more viscous, making the resulting particle smaller [42].

While these nano-HKUST-1 could exhibited the typical octahedral morphology of HKUST-1, suggesting the successful formation of HKUST-1, it would be necessary to further identify crystalline structures of these nano-HKUST-1 in Fig. 3. Although various MWs of PVP were introduced to the syntheses of HKUST-1, H_3BTC was still well coordinated with Cu in each case, and all nano-HKUST-1 exhibited identical XRD patterns to that of the typical HKUST-1 [38,39], confirming that the addition of PVP would not destroy coordination between Cu^{2+} and H_3BTC to form HKUST-1.

On the other hand, even though the XRD patterns of nano-HKUST-1 were identical to that of the conventional one, surficial chemistry of these nano-HKUST-1 was then analyzed by IR, and the IR spectra of the pristine PVP with various MWs were also measured and displayed in Fig. 4(a). Specifically, the board peak located at 2926 and 3434 cm^{-1}, which can be indexed to stretching vibration of -CH_2 and -OH. The peaks at 1018 and 1285 cm^{-1} were assigned to C-N stretching vibration, and the peak at 1660 cm^{-1} was attributed to C═O stretching vibration. Fig. 4(b) further reveals IR spectra of nano-HKUST-1 prepared with PVP, and the signature peaks of HKUST-1 can be all detected at 1375 cm^{-1} corresponding to C—O, and 1450 cm^{-1} to C═O owing to the existence of BTC [43,44]. In addition, several noticeable peaks can be also detected at 1018, 1285, 2926, and 3434 cm^{-1}, suggesting that PVP was present on surfaces of these nano-HKUST-1, and PVP in fact would interact with Cu^{2+} during the synthesis of HKUST-1. More importantly, the original peak at 1660 cm^{-1} ascribed to the C═O stretching vibration would

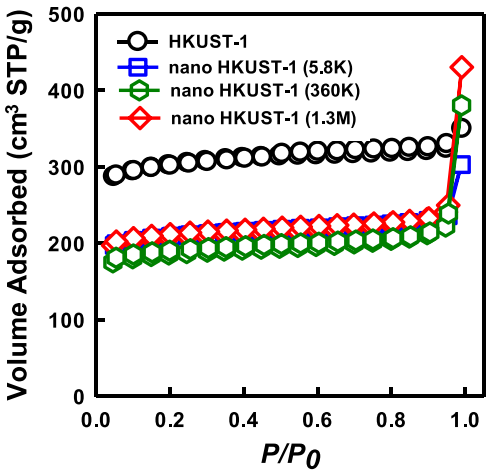

Fig. 5. N_2 sorption amount isotherms of HKUST-1 prepared with and without PVP.

notably shift toward lower wavenumbers as depicted in Fig. 4(c).

This was because the free carbonyl group (C═O) in the pyrrolidone ring of PVP would coordinated with Cu^{2+} via a weak chemical coordination [45]. As a result, the absorption peak would slightly shift toward lower wavenumbers [46,47]. More interestingly, it can be deduced in Fig. 4(c) that the order of the coordination interaction between Cu^{2+} and PVP with various MWs occur as follows: PVP = 1.3 M > PVP= 360k > PVP= 58k. On the other hand, the peak located at 1018 and 1285 cm^{-1} did not shift, indicating that the coordination of Cu^{2+} with O atom was much stronger than N atom, leading to a stronger steric influence and causing unable status to aggregate together during synthesis of HKUST-1 [48,49].

These features validate that PVP was deposited into these nano-HKUST-1 particles. As PVP is a hydrophilic polymer [50,51], and the solvent employed here for VL conversion was IPA, the existence of PVP on nano-HKUST-1 would facilitate dispersion of these PVP-deposited nano-HKUST-1 in IPA for improving VL oxidative reactions.

Furthermore, since the particle size of nano-HKUST-1 was significantly altered by the addition of PVP, the textural properties of these nano-HKUST-1 were then further analyzed. Fig. 5 presents N_2 sorption isotherms of the conventional HKUST-1 and the nano-HKUST-1. Essentially, these N_2 isotherms exhibited a similar pattern, and thus could be classified as the IUPAC type I isotherm. The specific surface area for the conventional HKUST-1 was 931.8 m^2/g, while the specific surface area of nano-HKUST-1 prepared by PVP = 5.8 K, 360 K and 1.3 M was decreased to 637.6, 568.5 and 640.0 m^2/g, respectively.

The existence of PVP seemed to reduce the specific surface area of nano-HKUST-1, while the size of nano-HKUST-1 was actually smaller. This reduction of specific surface area might be related to the deposition of PVP on nano-HKUST-1 surface and even encapsulated within pores of HKUST-1, restraining N_2 adsorption, and leading to the lower surface area. Previous studies have also indicated that smaller MOFs might

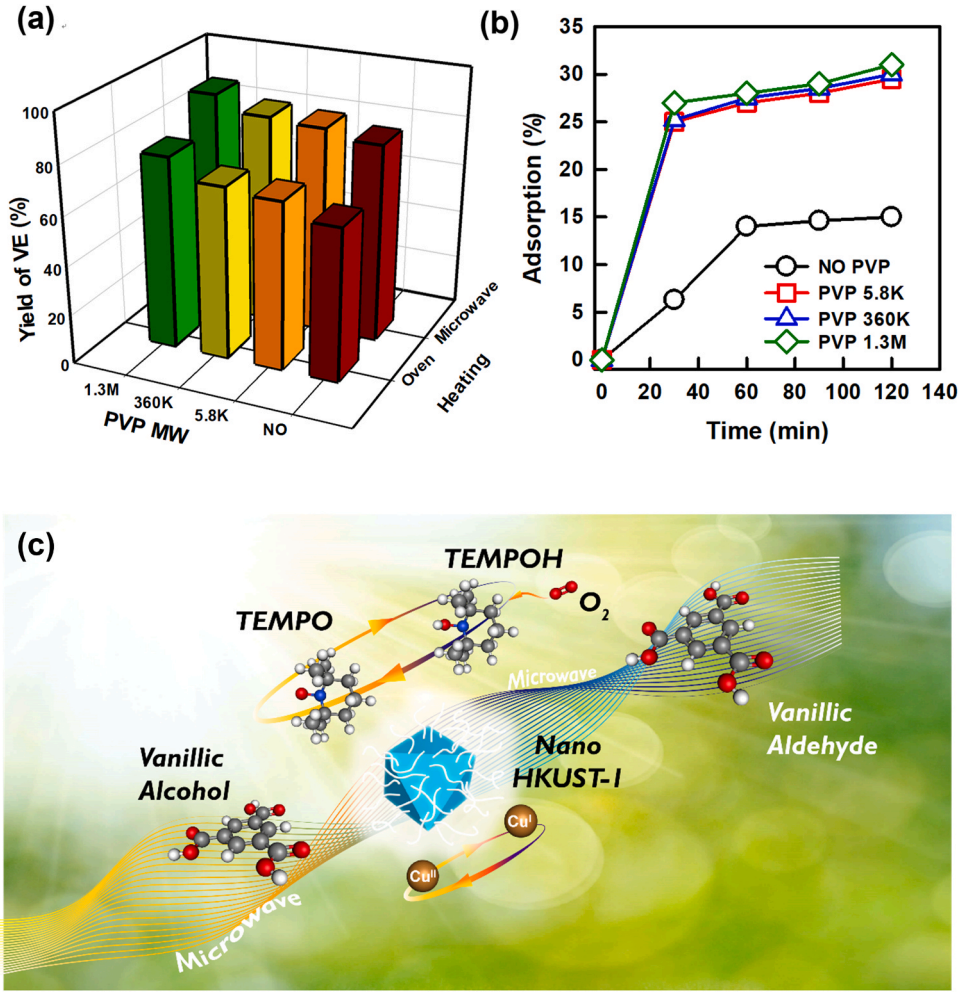

Fig. 6. (a) Conversion of VL to VE using HKUST-1 prepared with and without PVP under microwave irradiation and oven-heating (T = 120 °C, t = 120 min), (b) VL adsorption to HKUST-1 prepared with and without PVP at 25 °C; (c) a scheme for catalytic conversion of VL to VE using nano-HKUST-1 under microwave irradiation.

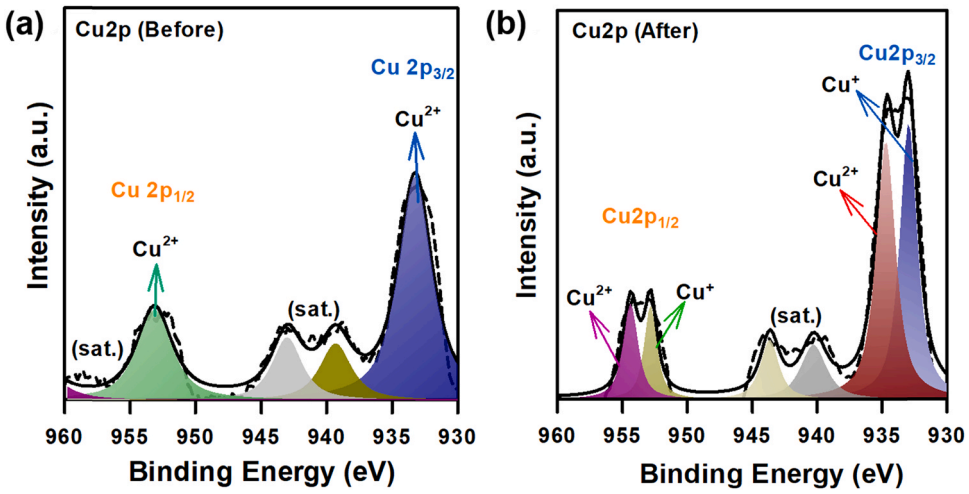

Fig. 7. XPS spectra of (a) the pristine nano-HKUST-1(1.3 M) and (b) the used nano-HKUST-1(1.3 M).

possess relatively low internal surfaces, leading to smaller surface areas [52]. Nevertheless, as the size of nano-HKUST-1 became smaller, its specific surface area would be also become higher. Thus, when these two factors took effects simultaneously, the specific surface area of nano-HKUST-1 firstly became smaller, and then raised up slightly at increasing MW of PVP.

3.2. Conversion of VL to VE using nano-HKUST-1

Fig. 6(a) shows yields of VE converted from VL by the conventional HKUST-1 and nano-HKUST-1. Since conversion of VL to VE is a thermo-chemical reaction, two heating methods were employed and compared: the oven-heating and microwave irradiation. In the case of oven-heating, when the conventional HKUST-1 (i.e., "NO" in Fig. 6(a)) was employed by oven-heating, a yield of VE (Y_{VE}) of 62.3% (i.e., C_{VL} = 62.3%, and S_{VE} = 100%) can be obtained, demonstrating that the conventional HKUST-1 could incorporate with TEMPO to oxidize VL to VE selectively. Subsequently, when nano-HKUST-1(5.8 K) was employed, Y_{VE} was noticeably increased from 62.3% to 68.3%. In the cases of nano-HKUST-1(360 K) and nano-HKUST-1(1.3 M), their corresponding Y_{VE} could be noticeably increased to 70.1%, and 78%, respectively, demonstrating that nano-HKUST-1 seemed to exhibit higher catalytic activities than the conventional HKUST-1 for oxidation of VL to VE. Especially, when a higher MW of PVP was employed for preparing nano-HKUST-1, a higher Y_{VE} can be obtained.

On the other hand, when microwave irradiation was employed to replace oven-heating, the corresponding Y_{VE} obtained by the conventional HKUST-1 was 80.6% (i.e., C_{VL} = 80.6%, and S_{VE} = 100%), showing that microwave irradiation could significantly improve VL conversion to VE. Moreover, when nano-HKUST-1(5.8 K) was employed, Y_{VE} could be increased from 80.6% to 83.8%. In the cases of nano-HKUST-1(360 K) and nano-HKUST-1(1.3 M), their corresponding Y_{VE} under microwave irradiation could be also considerably increased to 85% and 91%, respectively.

These comparisons further demonstrated that the heating method was a critical factor for oxidation of VL to VE, and microwave irradiation appeared as a much more effective method than oven-heating for conversion of VL to VE because microwave irradiation could provide a more efficient heating process for rapid and intense heat from the interior of catalyst [53,54]. Additionally, metal-oxide moiety could absorb heat more rapidly under microwave irradiation to enhance reactions between HKUST-1, and VL [55]. The ligand of HKUST-1 (i.e., BTC) might also absorb microwave irradiation and promote catalytic activities of Cu–O groups [20].

Since HKUST-1 and nano-HKUST-1 comprised of Cu-O cluster, this Cu-O cluster has been validated to play an important role in VL oxidation. Thus, XPS analyses of Cu2p of nano-HKUST-1(1.3 M) before and after VL oxidation were conducted. Fig. 7(a) exhibits two significant peaks at 933.3 and 953.1 eV, corresponding to Cu^{2+} of $Cu2p_{3/2}$ and $Cu2p_{1/2}$, respectively [56]. After VL oxidation, the Cu2p XPS spectrum of the used nano-HKUST-1 (Fig. 7(b)) showed a slightly different spectrum in which not only Cu^{2+} at 934.6 and 954.3 eV but also Cu^{+} species at 932.4 and 952.2 eV [57]. This suggests that the Cu-O cluster of nano-HKUST-1 indeed participated in VL oxidation, and the redox reaction between Cu^{2+} and Cu^{+} led to the formation of a reactive intermediate of VL [12,16,18,19,21,22] as illustrated in Fig. S1. Subsequently, TEMPO would then react with the intermediate of VL to withdraw a proton, producing TEMPOH and the product, VE [58,59]. The resultant TEMPOH was then converted back to TEMPO upon exposure to O_2 [30,40]. Through the cyclic process of TEMPO, VL could be continuously oxidized to VE selectively as illustrated in Fig. 6(c) [60].

More importantly, these results also validate that nano-HKUST-1 certainly possessed higher catalytic activities than the conventional HKUST-1 for oxidation of VL to VE, and a higher MW of PVP involved in nano-HKUST-1 would lead to a much higher Y_{VE}. Such a feature might be attributed to a number of possibilities. Firstly, even though the specific surface areas of these nano-HKUST-1 measured by N_2 sorption isotherms did not change significantly with MW of PVP, outer surfaces of octahedral nano-HKUST-1 would be definitely different because of various sizes. A smaller octahedral particle would certainly afford a much higher outer surface area which allows more reactive surfaces. Especially, when nano-HKUST-1 was immersed in liquids, liquid molecules would fill into the pores of nano-HKUST-1 [25], and then the outer surface would become critical for reactions. Therefore, the smaller nano-HKUST-1 obtained by higher MW of PVP would lead to a much higher conversion efficiency of VL to VE.

Secondly, as PVP in fact would be deposited into nano-HKUST-1, the hydrophilic PVP might increase affinity of VL towards to HKUST-1 for facilitating reactions between VL and nano-HKUST-1. To further probe into the affinity between VL and HKUST-1 or nano-HKUST-1, adsorption of VL to HKUST-1 and nano-HKUST-1 was investigated especially at ambient temperature to avoid thermo-chemical conversion of VL in Fig. 6(b). In the case of the conventional HKUST-1, 6.5% of the added VL had been adsorbed onto HKUST-1 at 30 min; the adsorption increased to 14.5% at 60 min, and then 15% afterwards. Interestingly, in the case of nano-HKUST-1(5.8 K), VL could be also adsorbed to it, exhibiting an adsorption of 25.0% at 30 min; subsequently, the adsorption also gradually increased to 29.5% at 120 min. Similar trends can be also observed in the cases of nano-HKUST-1(360 K), and nano-HKUST-1 (1.3 M). These results validate that the affinity of VL towards nano-

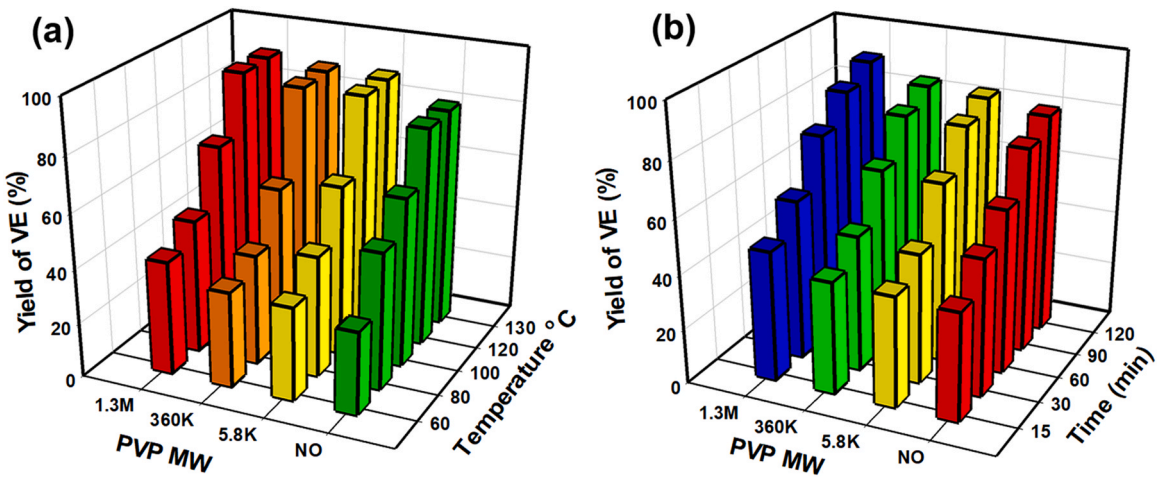

Fig. 8. Effects of (a) temperatures and (b) reaction time on conversion of VL to VE by HKUST-1, and nano-HKUST-1.

HKUST-1 was much stronger than that towards the conventional HKUST-1. More importantly, the adsorption to nano-HKUST-1 had been almost four times more than that to the conventional HKUST-1, indicating that the presence of PVP would certainly facilitate the interaction between VL and nano-HKUST-1 to enhance the VL oxidative reaction.

Therefore, these results successfully demonstrate that synthesis of HKUST-1 would be mediated by the addition of PVP to afford much smaller HKUST-1 particles and also enable the surficial properties of HKUST-1 more favorable for reacting with VL.

3.3. Effects of time and temperature on VL oxidation

As nano-HKUST-1 had been validated to achieve a much higher conversion efficiency of VL to VE by mediated with PVP especially under microwave irradiation, it would be essential to further investigate effects of time and temperature of such a thermos-chemical reaction of VL oxidation. Fig. 8(a) displays the effect of reaction temperature on VL conversion to VE using various HKUST-1. In the case of the conventional HKUST-1 (i.e., "NO" PVP), when a much lower temperature of 60 °C was employed, VL could be still converted to VE with Y_{VE} = 30.5% (C_{VL} = 30.5%, S_{VE} = 100% as listed in Table S1). At increasing temperatures from 60° to 130°C, Y_{VE} considerably increased from 30.5% to 81% while S_{VE} remained 100% throughout the tested range of temperatures.

On the other hand, when nano-HKUST-1(5.8 K) was employed at 60 °C, the corresponding Y_{VE} was 34.5%, which also significantly increased along with the elevated temperatures to 89% at 130 °C. Similar results can be observed in the cases of nano-HKUST-1(360 K), and nano-HKUST-1(1.3 M) as Y_{VE} was 35.2% and 41.8% at 60 °C, increasing to 89.5% and 91.1% at 130 °C, respectively. These results further validated that a relatively low temperature such as 60 °C would still allow nano-HKUST-1 to exhibit higher VL conversion efficiencies than the conventional HKUST-1, and a higher temperature would enable a higher Y_{VE} while maintaining S_{VE} of 100%.

On the other hand, the effect of reaction time on VL conversion had been also investigated to vary the reaction duration from 15 to 120 min in Fig. 8(b). When the reaction duration was short as 15 min at 120 °C, VL could be still converted to afford Y_{VE} = 33.9% by the conventional HKSUT-1. Once the reaction duration was increased from 15 to 30, 60, 90, and 120 min, the corresponding Y_{VE} was considerably raised up from 33.9 to 50.3, 60.1, 75.1, and then 80.6%, respectively, showing that the longer reaction duration would certainly enhance VL conversion to VE. In the case of nano-HKUST-1(5.8 K), a slightly higher Y_{VE} (40.6%) than the conventional HKUST-1 could be achieved after a duration of 15 min, and then considerably increased from 40.6% to 47.6%, 65.6%, 79.6%, and 83.8% after 30, 60, 90, and 120 min, respectively. Similar results can be obtained by nano-HKUST-1(360 K), and nano-HKUST-1(1.3 M) as Y_{VE} could be increased from 41.1%, and 47.6% at 15 min, to 85.0%, and 91.0% at 120 min, respectively. These results validated that a longer reaction duration would certainly benefit VL conversion as VL conversion would considerably increase. More importantly, there was no VC detected and S_{VE} maintained 100% even after a longer duration, suggesting that no over-oxidation of VE occurred by this nano-HKUST-1/TEMPO system. On the other hand, these results also confirm that nano-HKUST-1 prepared by a higher MW of PVP would certainly lead to a higher Y_{VE}, validating the advantagous mediating effect of PVP with higher MWs.

Table 1
VL to VE catalyzed by using various oxidation techniques.

Catalyst	Oxidant	Temp. (°C)	VL Con. (%)	VE Sel. (%)	VE Yield (%)	Ref.
Nano-HKUST-1 (1.3 M)	**air**	**120**	**91**	**100**	**91**	**This study**
CuO/ $MgAl_2O_4$	H_2O_2	90	67	74		[61]
CuO/ $MgFe_2O_4$			53	46		
MnFe	O_2	100	21	79	21	[62]
FeFe			70	91	31	
CoFe			70	84	5	
NiFe			76	11	5	
CuFe			86	35	5	
ZnFe			46	19	15	
Au-Pd	air	30	52.8	49.6	26.2	[63]
N-RGO/ Mn_3O_4	air	120	26.4	19.2	5.1	[64]
nCo-MO	air	120	7.0	5.7	0.4	[65]
Co_3O_4	air	120	47.9	60.6	29	[66]
$MnCl_2$	H_2O_2	75	38	19	7.2	[1]
	H_2O_2	75	28	5	1.4	
	H_2O_2	80	89.6	49.4	44.3	
$CrCl_3$	H_2O_2	80	94.2	60.6	57.1	
$CoCl_2$	H_2O_2	80	48.1	33.9	16.3	

To further compare VL conversion efficiency by this nano-HKUST-1/TEMPO system with literatures, Table 1 lists VL conversion efficiencies of this study, and other reported values. One can notice that nano-HKUST-1/TEMPO outperformed than many reported conversion efficiencies by other catalytic oxidation processes as listed in Table 1, including many noble-metal-involved processes. This comparison clearly validates that nano-HKUST-1 is a promising heterogeneous catalyst for oxidizing VL into VE.

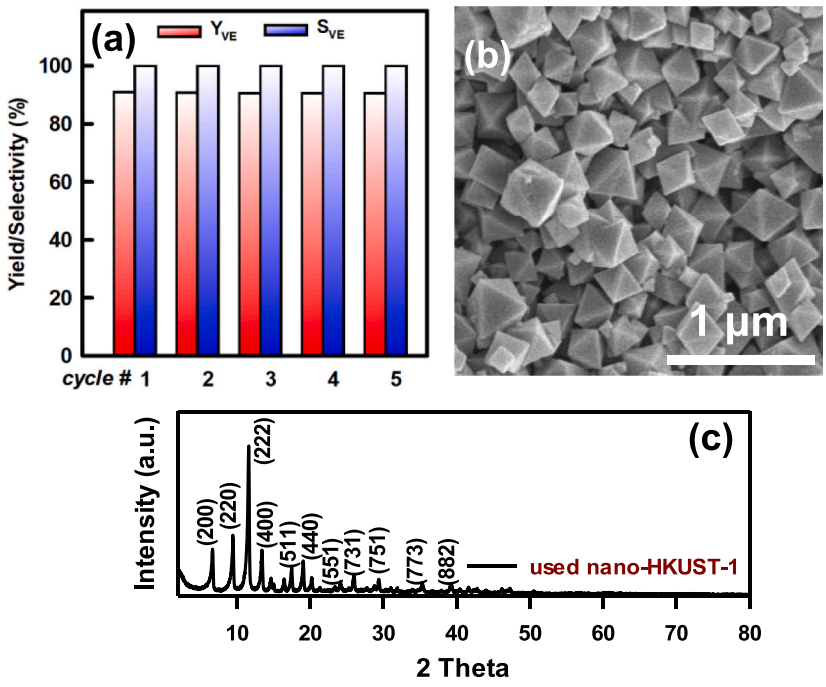

Fig. 9. (a) Recyclability of nano-HKUST-1(1.3 M) on conversion of VL to VE. (T = 120 °C, t = 120 min); (b) SEM image and (c) XRD of used nano-HKUST-1(1.3 M).

3.4. Recyclable of nano-HKUST-1

As nano-HKUST-1 was proposed as a heterogeneous catalyst for converting VL to VE, its recyclability was crucial and thus tested. Fig. 9 (a) shows a series of VL conversion efficiencies at 120 °C for 120 min by reusing nano-HKUST-1(1.3 M) for 5 cycles without any regeneration treatments. VL could be consistently oxidized and converted to VE without noticeable variation in Y_{VE}, and S_{VE}. This demonstrates that nano-HKUST-1 could be reusable to exhibit a stable catalytic activity towards oxidation of VL to VE. Fig. 9(b) also displays a SEM image of used nano-HKUST-1 which still exhibited a well-defined octahedral morphology, and the corresponding XRD pattern could be also well-indexed to the pristine HKUST-1, validating that nano-HKUST-1 was a certainly reusable, and durable catalyst.

4. Conclusion

In this study, the conventional micrometer-scaled HKUST-1 was particularly fabricated into nanoscale HKUST-1 by introducing PVP as a capping agent. These nano-HKUST-1 not only retained the crystalline structure of HKUST-1 but also maintained the classic octahedral morphology of HKUST-1 for the first time in literature. More importantly, the size of nano-HKUST-1 can be further mediated and manipulated by chaning MW of PVP. In particular, when the conventional HKUST-1 prepared without PVP exhibited an average size of 2800 nm, introduction of PVP= 5.8 K into HKUST-1 synthesis would decrease the size to 480 nm, whereas usage of PVPMW=360 K and PVPMW=1.3 M would afford nano-HKUST-1 with 310 nm, and 170 nm, respectively. Interestingly, the introduced PVP would not just alter the size of HKUST-1 through the capping effect but also deposit PVP molecules into these nano-HKUST-1, increasing hydrophilicity of nano-HKUST-1 to attract VL in solvents. Thus, nano-HKUST-1 could exhibit noticeably higher VL conversion efficiencies then the conventional HKUST-1 owing to the smaller size of nano-HKUKST-1 for providing more reactive outer surface, and the more hydrophilic surficial properties of nano-HKUST-1 for increasing stronger affinity towards reactants. In addition, nano-HKUST-1 can be also employed for VL conversion to VE with 100% of selectivity even at a very short reaction time of 15 min and a very low temperature of 60 °C. Moreover, nano-HKUST-1 could also exhibit a high Y_{VE}=91% with S_{VE}=100% at 120 °C for 120 min, and such a VL conversion efficiency already outperformed many other reported values even by noble-metal-catalysts. Nano-HKUST-1 can be also reusable and exhibit stable Y_{VE} and 100% of S_{VE}. These features all indicate that nano-HKUST-1 prapred by mediation of PVP is certainly a more advantageous heterogeneous Cu-based catalyst for converting VL to VE, and the mediating effect of PVP revealed here also gives insights to further engieer other MOFs materials for enhancing their applications.

CRediT authorship contribution statement

Bing-Cheng Li: Data curation, Writing – original draft; Jia-Yin Lin: Data curation; Jechan Lee: Data curation, Visualization, Investigation; Eilhann Kwon: Data curation, Visualization, Investigation; Bui Xuan Thanh: Writing – review & editing; Xiaoguang Duan: Writing – original draft, Hsing Hua Chen: Data curation, Visualization Investigation; Hongta Yang: Writing – review & editing, Kun-Yi Andrew Lin: Data curation, Writing – original draft.

Declaration of Competing Interest

The authors declare that they have no known competing financial interests or personal relationships that could have appeared to influence the work reported in this paper.

Acknowledgements

This work is supported by the Ministry of Science and Technology (MOST) (110-2636-E-005-003), Taiwan, and financially supported by the “Innovation and Development Center of Sustainable Agriculture” from The Featured Areas Research Center Program within the framework of the Higher Education Sprout Project by the Ministry of Education (MOE), Taiwan. The authors gratefully acknowledge the use of EA003600/SQUID000200 of MOST 110-2731-M-006-001 belonging to the Core Facility Center of National Cheng Kung University.

Appendix A. Supporting information

Supplementary data associated with this article can be found in the online version at doi:10.1016/j.colsurfa.2021.127639.

References

[1] J. Pan, J. Fu, X. Lu, Microwave-assisted oxidative degradation of lignin model compounds with metal salts, Energy Fuels 29 (2015) 4503–4509.
[2] S. Saha, S.B.A. Hamid, T.H. Ali, Catalytic evaluation on liquid phase oxidation of vanillyl alcohol using air and H_2O_2 over mesoporous Cu-Ti composite oxide, Appl. Surf. Sci. 394 (2017) 205–218.
[3] Z. Yuan, S. Chen, B. Liu, Nitrogen-doped reduced graphene oxide-supported Mn_3O_4: an efficient heterogeneous catalyst for the oxidation of vanillyl alcohol to vanillin, J. Mater. Sci. 52 (2017) 164–172.
[4] M. Fache, B. Boutevin, S. Caillol, Vanillin production from lignin and its use as a renewable chemical, ACS Sustain. Chem. Eng. 4 (2016) 35–46.
[5] R. Yepez, S. Garcia, P. Schachat, M. Sanchez-Sanchez, J.H. Gonzalez-Estefan, E. Gonzalez-Zamora, I.A. Ibarra, J. Aguilar-Pliego, Catalytic activity of HKUST-1 in the oxidation of trans-ferulic acid to vanillin, N. J. Chem. 39 (2015) 5112–5115.
[6] P. Elamathi, M.K. Kolli, G. Chandrasekar, Catalytic oxidation of vanillyl alcohol using FeMCM-41 nanoporous tubular reactor, Int. J. Nanosci. 17 (2017).
[7] J.G. Flores, E. Sánchez-González, A. Gutiérrez-Alejandre, J. Aguilar-Pliego, A. Martínez, T. Jurado-Vázquez, E. Lima, E. González-Zamora, M. Díaz-García, M. Sánchez-Sánchez, I.A. Ibarra, Greener synthesis of Cu-MOF-74 and its catalytic use for the generation of vanillin, Dalton Trans. 47 (2018) 4639–4645.
[8] K.-Y.A. Lin, H.-K. Lai, Z.-Y. Chen, Selective generation of vanillin from catalytic oxidation of a lignin model compound using ZIF-derived carbon-supported cobalt nanocomposite, J. Taiwan Inst. Chem. Eng. 78 (2017) 337–343.
[9] H.-K. Lai, Y.-Z. Chou, M.-H. Lee, K.-Y.A. Lin, Coordination polymer-derived cobalt nanoparticle-embedded carbon nanocomposite as a magnetic multi-functional catalyst for energy generation and biomass conversion, Chem. Eng. J. 332 (2018) 717–726.
[10] K.-Y.A. Lin, H.-K. Lai, Z.-Y. Chen, Selective generation of vanillin from catalytic oxidation of a lignin model compound using ZIF-derived carbon-supported cobalt nanocomposite, J. Taiwan Inst. Chem. Eng. 78 (2017) 337–343.
[11] N.J. Hill, J.M. Hoover, S.S. Stahl, Aerobic alcohol oxidation using a copper(I)/TEMPO catalyst system: a green, catalytic oxidation reaction for the undergraduate organic chemistry laboratory, J. Chem. Educ. 90 (2013) 102–105.
[12] J.M. Hoover, B.L. Ryland, S.S. Stahl, Mechanism of copper(I)/TEMPO-catalyzed aerobic alcohol oxidation, J. Am. Chem. Soc. 135 (2013) 2357–2367.
[13] S.A. Tromp, I. Matijošytė, R.A. Sheldon, I.W.C.E. Arends, G. Mul, M.T. Kreutzer, J. A. Moulijn, S. deVries, Mechanism of laccase–TEMPO-catalyzed oxidation of benzyl alcohol, ChemCatChem 2 (2010) 827–833.
[14] N. Wang, R. Liu, J. Chen, X. Liang, $NaNO_2$-activated, iron–TEMPO catalyst system for aerobic alcohol oxidation under mild conditions, Chem. Commun. (Camb., Engl.) (2005) 5322–5324.
[15] S. Gharehkhani, Y. Zhang, P. Fatehi, Lignin-derived platform molecules through TEMPO catalytic oxidation strategies, Prog. Energy Combust. Sci. 72 (2019) 59–89.
[16] P. Tan, Y. Jiang, X.-Q. Liu, D.-Y. Zhang, L.-B. Sun, Magnetically responsive core–shell Fe_3O_4@C adsorbents for efficient capture of aromatic sulfur and nitrogen compounds, ACS Sustain. Chem. Eng. 4 (2016) 2223–2231.
[17] J.Y. Lin, B.X. Thanh, E. Kwon, K.Y.A. Lin, Enhanced Catalytic Conversion of 5-Hydroxymethylfurfural to 2,5-Diformylfuran by HKUST-1/TEMPO Under Microwave Irradiation.
[18] M.W. Zheng, K.Y.A. Lin, C.H. Lin, TEMPO-Functionalized Silica as an Efficient and Recyclable Oxidation Catalyst for Conversion of a Lignin Model Compound to Value-Added Products. Waste Biomass Valor 11, 6917–6928 (2020).
[19] J.-Y. Lin, K.-Y.A. Lin, Catalytic conversion of a lignin model compound to value-added products using Cu/TEMPO-catalyzed aerobic oxidation, Biomass Convers. Biorefinery 9 (2019) 617–623.
[20] J.-Y. Lin, B.X. Thanh, E. Kwon, K.-Y.A. Lin, Enhanced catalytic conversion of 5-hydroxymethylfurfural to 2,5-diformylfuran by HKUST-1/TEMPO under microwave irradiation, Biomass Convers. Biorefinery (2020).
[21] J.-Y. Lin, H. Wang, W.D. Oh, J. Lee, E. Kwon, S. You, C.-H. Lin, K.-Y.A. Lin, Integrated MOF-mesh and TEMPO-grafted carbon fiber as a sandwich-like catalytic system for selective valorization of lignin-derived compound under microwave irradiation, Chem. Eng. J. 411 (2021), 128605.
[22] J.-Y. Lin, F. Ghanbari, Y.S. Ok, G. Lisak, K.-Y.A. Lin, F.-C. Chang, Selective aerobic upgrading of lignin-derived compound using a recyclable dual-functional TPO-loaded Cu-BTC catalyst, Waste Biomass Valoriz. 12 (2021) 673–685.
[23] K.-Y. Andrew Lin, Y.-T. Hsieh, Copper-based metal organic framework (MOF), HKUST-1, as an efficient adsorbent to remove p-nitrophenol from water, J. Taiwan Inst. Chem. Eng. 50 (2015) 223–228.
[24] I. Senkovska, S. Kaskel, Ultrahigh porosity in mesoporous MOFs: promises and limitations, Chem. Commun. 50 (2014) 7089–7098.
[25] T.M. Osborn Popp, A.Z. Plantz, O.M. Yaghi, J.A. Reimer, Precise control of molecular self-diffusion in Isoreticular and multivariate metal-organic frameworks, Chemphyschem 21 (2020) 32–35.
[26] J.-Y. Lin, M.-H. Yuan, K.-Y.A. Lin, C.-H. Lin, Selective aerobic oxidation of 5-hydroxymethylfurfural to 2,5-diformylfuran catalyzed by Cu-based metal organic frameworks with 2,2,6,6-tetramethylpiperidin-oxyl, J. Taiwan Inst. Chem. Eng. 102 (2019) 242–249.
[27] F. Zou, R. Yu, R. Li, W. Li, Microwave-assisted synthesis of HKUST-1 and functionalized HKUST-1-@$H_3PW_{12}O_{40}$: selective adsorption of heavy metal ions in water analyzed with synchrotron radiation, Chemphyschem 14 (2013) 2825–2832.
[28] J.-Y. Lin, H.-K. Lai, K.-Y.A. Lin, Rapid microwave-hydrothermal conversion of lignin model compounds to value-added products via catalytic oxidation using metal organic frameworks, Chem. Pap. 72 (2018) 2315–2325.
[29] Y. Liu, B. Liu, Q. Zhou, T. Zhang, W. Wu, Morphology effect of metal-organic framework HKUST-1 as a catalyst on benzene oxidation, Chem. Res. Chin. Univ. 33 (2017) 971–978.
[30] Y. Chen, J. Zhang, M. Zhang, X. Wang, Molecular and textural engineering of conjugated carbon nitride catalysts for selective oxidation of alcohols with visible light, Chem. Sci. 4 (2013) 3244–3248.
[31] Z.-Q. Li, L.-G. Qiu, T. Xu, Y. Wu, W. Wang, Z.-Y. Wu, X. Jiang, Ultrasonic synthesis of the microporous metal–organic framework $Cu_3(BTC)_2$ at ambient temperature and pressure: An efficient and environmentally friendly method, Mater. Lett. 63 (2009) 78–80.
[32] J. Li, K. Inukai, Y. Takahashi, A. Tsuruta, W. Shin, Effect of PVP on the synthesis of high-dispersion core–shell barium-titanate–polyvinylpyrrolidone nanoparticles, J. Asian Ceram. Soc. 5 (2018) 216–225.
[33] S. Wang, Y. Lv, Y. Yao, H. Yu, G. Lu, Modulated synthesis of monodisperse MOF-5 crystals with tunable sizes and shapes, Inorg. Chem. Commun. 93 (2018) 56–60.
[34] S.S.-Y. Chui, S.M.-F. Lo, J.P.H. Charmant, A.G. Orpen, I.D. Williams, A chemically functionalizable nanoporous material $[Cu_3(TMA)_2(H_2O)_3]n$, Science 283 (1999) 1148–1150.
[35] K.-Y.A. Lin, H. Yang, C. Petit, F.-K. Hsu, Removing oil droplets from water using a copper-based metal organic frameworks, Chem. Eng. J. 249 (2014) 293–301.
[36] M.-W. Zheng, K.-Y.A. Lin, C.-H. Lin, TEMPO-functionalized silica as an efficient and recyclable oxidation catalyst for conversion of a lignin model compound to value-added products, Waste Biomass Valoriz. 11 (2020) 6917–6928.
[37] J.-Y. Lin, J. Lee, K.-Y.A. Lin, Microwave-assisted catalyst-free oxidative conversion of a lignin model compound to value-added products using TEMPO, Waste Biomass Valoriz. 11 (2019) 3621–3628.
[38] J.-Y. Lin, M.-H. Yuan, K.-Y.A. Lin, C.-H. Lin, Selective aerobic oxidation of 5-hydroxymethylfurfural to 2,5-diformylfuran catalyzed by Cu-based metal organic frameworks with 2,2,6,6-tetramethylpiperidin-oxyl, J. Taiwan Inst. Chem. Eng. 102 (2019) 242–249.
[39] L. Zhou, Z. Niu, X. Jin, L. Tang, L. Zhu, Effect of lithium doping on the structures and CO_2 adsorption properties of metal-organic frameworks HKUST-1, ChemistrySelect 3 (2018) 12865–12870.
[40] P. Tan, X.Y. Xie, X.Q. Liu, T. Pan, C. Gu, P.F. Chen, J.Y. Zhou, Y. Pan, L.B. Sun, Fabrication of magnetically responsive HKUST-1/Fe_3O_4 composites by dry gel conversion for deep desulfurization and denitrogenation, J. Hazard Mater. 321 (2017) 344–352.
[41] I.A. Safo, M. Werheid, C. Dosche, M. Oezaslan, The role of polyvinylpyrrolidone (PVP) as a capping and structure-directing agent in the formation of Pt nanocubes, Nanoscale Adv. 1 (2019) 3095–3106.
[42] N. Izu, I. Matsubara, T. Itoh, W. Shin, M. Nishibori, Controlled synthesis of monodispersed cerium oxide nanoparticle sols applicable to preparing ordered self-assemblies, Bull. Chem. Soc. Jpn. 81 (2008) 761–766.
[43] N.A. Gomez, R. Abonia, H. Cadavid, I.H. Vargas, Chemical and spectroscopic characterization of a vegetable oil used as dielectric coolant in distribution transformers, J. Braz. Chem. Soc. 22 (2011) 2292–2303.
[44] L. Peng, J. Zhang, J. Li, B. Han, Z. Xue, B. Zhang, J. Shi, G. Yang, Hollow metal–organic framework polyhedra synthesized by a CO_2–ionic liquid interfacial templating route, J. Colloid Interface Sci. 416 (2014) 198–204.
[45] B.Z. Zongtao Zhang, Liming Hu, PVP protective mechanism of ultrafine silver powder synthesized by chemical reduction processes, J. Solid State Chem. 121 (1996) 105–110.
[46] T. Morioka, M. Takesue, H. Hayashi, M. Watanabe, R.L. Smith Jr., Antioxidation properties and surface interactions of polyvinylpyrrolidone-capped zerovalent copper nanoparticles synthesized in supercritical water, ACS Appl. Mater. Interfaces 8 (2016) 1627–1634.
[47] G. Granata, A. Onoguchi, C. Tokoro, Preparation of copper nanoparticles for metal-metal bonding by aqueous reduction with d-glucose and PVP, Chem. Eng. Sci. 209 (2019), 115210.
[48] D. Tomotoshi, H. Kawasaki, Surface and interface designs in copper-based conductive Inks for printed/flexible electronics, Nanomaterials (Basel) 10 (2020).
[49] M.W. Yuan-Jun Song, Xiao-Yang Zhang, Jing-Yuan Wu, Tong Zhang, Investigation on the role of the molecular weight of polyvinyl pyrrolidone in the shape control of high-yield silver nanospheres and nanowires, Nanoscale Res. Lett. 9 (2014) 17.
[50] L. Lv, Z. Li, Y. Ruan, Y. Chang, X. Ao, J.-G. Li, Z. Yang, C. Wang, Nickel-iron diselenide hollow nanoparticles with strongly hydrophilic surface for enhanced oxygen evolution reaction activity, Electrochim. Acta 286 (2018) 172–178.
[51] Y.J. Jo, E.Y. Choi, N.W. Choi, C.K. Kim, Antibacterial and hydrophilic characteristics of poly(ether sulfone) composite membranes containing zinc oxide nanoparticles grafted with hydrophilic polymers, Ind. Eng. Chem. Res. 55 (2016) 7801–7809.
[52] F. Wang, H. Guo, Y. Chai, Y. Li, C. Liu, The controlled regulation of morphology and size of HKUST-1 by "coordination modulation method", Microporous Mesoporous Mater. 173 (2013) 181–188.
[53] Z. Zhang, Z.K. Zhao, Microwave-assisted conversion of lignocellulosic biomass into furans in ionic liquid, Bioresour. Technol. 101 (2010) 1111–1114.
[54] C. Li, Z. Zhang, Z.K. Zhao, Direct conversion of glucose and cellulose to 5-hydroxymethylfurfural in ionic liquid under microwave irradiation, Tetrahedron Lett. 50 (2009) 5403–5405.

[55] T.-Y. Lin, K.-Y.A. Lin, Microwave-enhanced catalytic transfer hydrogenation of levulinic acid to γ-valerolactone using zirconium-based metal organic frameworks: a comparative study with conventional heating processes, J. Taiwan Inst. Chem. Eng. 96 (2019) 321–328.
[56] T. Wi-Afedzi, E. Kwon, D.D. Tuan, K.-Y.A. Lin, F. Ghanbari, Copper hexacyanoferrate nanocrystal as a highly efficient non-noble metal catalyst for reduction of 4-nitrophenol in water, Sci. Total Environ. 703 (2020), 134781.
[57] S.O. Thomas Waechtler, Nina Roth, Alexander Jakob, Heinrich Lang, Ramona Ecke, Stefan E. Schulz, Thomas Gessner, Anastasia Moskvinova, Steffen Schulze, Copper Oxide, Films grown by atomic layer deposition from bis (tri-n-butylphosphane)copper(I)acetylacetonate on Ta, TaN, Ru, and SiO_2, J. Electrochem. Soc. 156 (2009) H453–H459.
[58] A. Dhakshinamoorthy, M. Alvaro, H. Garcia, Aerobic oxidation of benzylic alcohols catalyzed by metal−organic frameworks assisted by TEMPO, ACS Catalysis 1 (2010) 48–53.
[59] N.J. Hill, J.M. Hoover, S.S. Stahl, Aerobic alcohol oxidation using a copper(I)/TEMPO catalyst system: a green, catalytic oxidation reaction for the undergraduate organic chemistry laboratory, J. Chem. Educ. 90 (2012) 102–105.
[60] W.-C. Yun, T.-Y. Lin, H.-Y. Chiu, K.-Y.A. Lin, Microwave irradiation-enhanced catalytic transfer hydrogenation of levulinic acid to γ-valerolactone using ruthenium: A comparative study with conventional heating processes, Waste Biomass Valoriz. 11 (2019) 2783–2793.
[61] B. Rahmanivahid, M. Pinilla-de Dios, M. Haghighi, R. Luque, Mechanochemical synthesis of $CuO/MgAl_2O_4$ and $MgFe_2O_4$ spinels for vanillin production from isoeugenol and vanillyl alcohol, Molecules 24 (2019).
[62] M.-W. Zheng, H.-K. Lai, K.-Y.A. Lin, Valorization of vanillyl alcohol by pigments: Prussian Blue analogue as a highly-effective heterogeneous catalyst for aerobic oxidation of vanillyl alcohol to vanillin, Waste Biomass Valoriz. (2018) 1–10.
[63] M. Wu, J.-H. Pang, P.-P. Song, J.-J. Peng, F. Xu, Q. Li, X.-M. Zhang, Visible light-driven oxidation of vanillyl alcohol in air with Au–Pd bimetallic nanoparticles on phosphorylated hydrotalcite, N. J. Chem. 43 (2019) 1964–1971.
[64] Z. Yuan, S. Chen, B. Liu, Nitrogen-doped reduced graphene oxide-supported Mn_3O_4: an efficient heterogeneous catalyst for the oxidation of vanillyl alcohol to vanillin, J. Mater. Sci. 52 (2016) 164–172.
[65] A. Jha, D. Mhamane, A. Suryawanshi, S.M. Joshi, P. Shaikh, N. Biradar, S. Ogale, C. V. Rode, Triple nanocomposites of $CoMn_2O_4$, Co_3O_4 and reduced graphene oxide for oxidation of aromatic alcohols, Catal. Sci. Technol. 4 (2014) 1771.
[66] R. Behling, G. Chatel, S. Valange, Sonochemical oxidation of vanillyl alcohol to vanillin in the presence of a cobalt oxide catalyst under mild conditions, Ultrason. Sonochem. 36 (2017) 27–35.